PAPER • OPEN ACCESS

EEG functional connectivity and deep learning for automatic diagnosis of brain disorders: Alzheimer's disease and schizophrenia

To cite this article: Caroline L Alves *et al* 2022 *J. Phys. Complex.* **3** 025001

View the article online for updates and enhancements.

You may also like

- A review of physiological and behavioral monitoring with digital sensors for neuropsychiatric illnesses
Erik Reinertsen and Gari D Clifford

- Green space structures and schizophrenia incidence in Taiwan: is there an association?
Hao-Ting Chang, Chih-Da Wu, Jung-Der Wang et al.

- Multiscale network dynamics between heart rate and locomotor activity are altered in schizophrenia
Erik Reinertsen, Supreeth P Shashikumar, Amit J Shah et al.

Journal of Physics: Complexity

PAPER

EEG functional connectivity and deep learning for automatic diagnosis of brain disorders: Alzheimer's disease and schizophrenia

Caroline L Alves[1,2,*], Aruane M Pineda[2], Kirstin Roster[2], Christiane Thielemann[1] and Francisco A Rodrigues[2]

[1] BioMEMS, Technische Hochschule Aschaffenburg, Aschaffenburg, Germany
[2] Universidade de São Paulo (USP), Instituto de Ciências Matemáticas e de Computação, São Carlos, SP, Brazil
[*] Author to whom any correspondence should be addressed.

E-mail: Caroline.Alves@th-ab.de and aruane.pineda@usp.br

Keywords: cortical networks, machine learning, complex networks, complex systems, deep learning

Abstract

Mental disorders are among the leading causes of disability worldwide. The first step in treating these conditions is to obtain an accurate diagnosis. Machine learning algorithms can provide a possible solution to this problem, as we describe in this work. We present a method for the automatic diagnosis of mental disorders based on the matrix of connections obtained from EEG time series and deep learning. We show that our approach can classify patients with Alzheimer's disease and schizophrenia with a high level of accuracy. The comparison with the traditional cases, that use raw EEG time series, shows that our method provides the highest precision. Therefore, the application of deep neural networks on data from brain connections is a very promising method for the diagnosis of neurological disorders.

1. Introduction

Neurological disorders, including Alzheimer's disease (AD) and schizophrenia (SZ), are among the main priorities in the present global health agenda [1]. AD is a type of dementia that affects primarily elderly individuals and is characterized by the degeneration of brain tissue, leading to impaired intellectual and social abilities [2]. Currently, around 25 million people live with AD [3]. In the US, nearly six million individuals are affected by AD, with incidence projected to increase more than two-fold to 13.8 million by 2050 [4]. Individuals with SZ have symptoms such as hallucinations, incoherent thinking, delusions, decreased intellectual functioning, difficulty in expressing emotions, and agitation [5, 6]. According to the World Health Organization, SZ affects around 26 million people worldwide [7].

The base for successful treatment of AD and SZ is the correct diagnosis. However, both the diagnosis and the determination of the stage of AD and SZ are based primarily on qualitative interviews, including psychiatric history and current symptoms, and the assessment of behavior. These observations may be subjective, imprecise, and incomplete [8–11]. To provide a quantitative evaluation of mental disorders, methods based on magnetic resonance imaging, computerized tomography [12], and positron emission tomography [13, 14] has been used to aid professionals in the diagnostic process [15]. However, the use of multiple imaging devices can be expensive to implement and the fusion of images from different devices can have poor quality due to motion artifacts.

To overcome these restrictions, EEG data is a viable candidate to support the diagnosis of SZ and AD [16]. Although EEG has a low spatial resolution, it has a comparatively low cost, good temporal resolution and is easily available in most contexts. Nonetheless, visual analysis of EEG data is time-consuming, requires specialized training, and is error-prone [17–19]. However, we can consider automatic evaluation of EEG time series using modern classification algorithms, which can help to improve the efficiency and accuracy of AD and SZ diagnosis, as verified in previous works [20–23].

Moreover, instead of using raw EEG time series, it is possible to encompass the connections between brain regions by constructing cortical complex networks [24]. In this case, we build cortical networks for healthy and individuals with neurological disorders. To distinguish between them, we use network measures to describe the network structure, as described in a previous work of ours [25] (see also [26, 27] for a description of the methodology used in network classification). Therefore, each network is mapped into a d dimensional space, where d is the number of measures adopted for network characterization. This process of building a set of features to represent the input data is called feature engineering. After extracting the network features for the two classes of networks, i.e. healthy and individuals with mental disorders, supervised learning algorithms are adjusted to perform automatic classification. Previous works verified that this approach enables the diagnosis with accuracy higher than 80% in the case of childhood-onset SZ [25].

Although this methodology has been used for many different diseases (e.g. [20, 25, 28, 29]) the performance of the algorithm depends on the measures selected to describe the network structure. The network properties included in the model could represent just a subset of the information necessary to get the best performance of the supervised model. Therefore, the network representation can be incomplete, restricting the accuracy of the classifiers. One possible solution to this problem is the use of a matrix of connections in combination with deep neural networks [30], as we show in the present paper. In this case, instead of extracting the network measures, the matrix of connections is considered as input to train a deep neural network. This matrix encodes all the information necessary to represent the network structure and avoid the choice of network measures.

In this work, the metrics used to construct the matrices also have restrictions. A limitation of the pairwise matrices used in this study is the possible loss of information when reducing the raw EEG time series. However, our study suggests that the amount of information retained is sufficient for the classification of AZ and SD and represents a more computationally efficient approach that is more practical in a clinical setting. In this work, the metrics used to construct the matrices also have restrictions. As an example, Pearson's correlation considers only linear correlations, on the other hand, Spearman's correlation is limited when there are many observations with the same order, and Granger's causality considers the series stationary. Nevertheless, we aim here to develop an efficient method to classify patients and not to make a comparison of methods.

Therefore, we consider the matrix of connections between brain areas and deep neural networks to distinguish individuals with AD and SZ from healthy controls. Other than previous works, where only raw time series are adopted as input for the neural network [31–37], we do not ignore the connections between the electrodes used to record the time series. We construct the matrix of connections by using Granger causality, Pearson's and Spearman's correlations [38–40]. We verify that this information about the connections is fundamental and improves the classification, compared to the previously mentioned approaches that use only raw EEG time series.

In summary, in this work we achieve the following contributions:

- We propose a method to classify EEG time series from healthy and patients presenting AD and SZ. With a matrix of connections as input for a tuned convolutional neural network (CNN) model, the accuracy obtained is close to 100% for both disorders. Our results are more accurate than those observed in previous works that consider only raw EEG time series, reinforcing the importance of the network structure on the diagnosis of mental disorders.

- We show that the method to infer the matrices of connections influences the quality of the classification results. For SZ, the Granger causality provides the most accurate classification, whereas, for AD, the Pearson's correlation yields the highest accuracy.

- Our framework is general and can be used in EEG data from any brain disorder. It allows to determine the best cortical network representation and adjust the CNN to optimize the accuracy.

In the next sections, we outline the data set, present the CNN architecture and show our results, comparing them with more common approaches that do not consider the connections between brain areas.

2. EEG data

The AD data set considered here is composed of EEG time series recorded at a sampling frequency of 128 Hz and a duration of 8 s for each individual and at 19 channels (F_{p1}, F_{p2}, F_7, F_3, F_z, F_4, F_8, T_3, C_3, C_z, C_4, T_4, T_5, P_3, P_z, P_4, T_6, O_1, and O_2). The letters F, C, P, O, and T refer to the respective cerebral lobes frontal (F), central (C), parietal (P), occipital (O), and temporal (T). The data is divided into two sets. The first one consists of 24 healthy elderly individuals (control group; aged 72 ± 11 years) who do not have any history of neurological disorders. The second one is made of 24 elderly individuals with AD (aged 69 ± 16 years) diagnosed by the National Institute of Neurological and Communicative Disorders and Stroke, the AD and Related Disorders Association, following the diagnostic and statistical manual of mental disorders (DSM)-III-R criteria ([20, 41]).
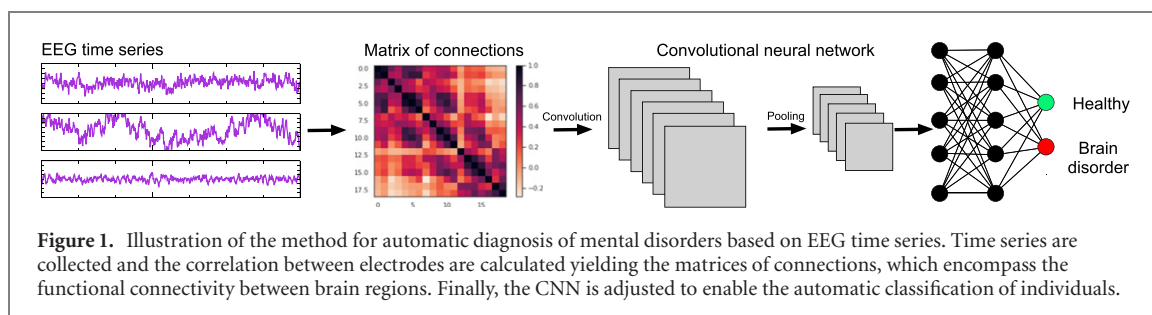
Figure 1. Illustration of the method for automatic diagnosis of mental disorders based on EEG time series. Time series are collected and the correlation between electrodes are calculated yielding the matrices of connections, which encompass the functional connectivity between brain regions. Finally, the CNN is adjusted to enable the automatic classification of individuals.

Table 1. Best hyperparameters and layer configurations obtained for the CNN$_{tuned}$ model.

Type of layer	Tuning hyperparameter	Value
Convolutional	—	—
Convolutional	Dropout	[0.00, 0.05, 0.10, 0.15, 0.20, 0.25, 0.30, 0.35, 0.40, 0.45, 0.50]
Convolutional	—	—
Convolutional	Number of filters	[32, 64]
Max pooling	Dropout	[0.00, 0.50, 0.10, 0.15, 0.20]
Flatten	—	—
Dense	-units-activation	[32, 64, 96, ..., 512] [relu, tanh, sigmoid]
Dropout	Rate	[0.00, 0.50, 0.10, 0.15, 0.20]
Adam optimization compile	Learning rate	Min $-$ value $= 1 \times 10^{-4}$ Max $-$ value $= 1 \times 10^{-2}$ Sampling $=$ LOG

Table 2. The network architecture for the CNN$_{tuned}$ model used in the AD and SZ data sets.

Type of layer	Output shape (AD)	Output shape (SZ)	Parameter
Convolutional	(None, 17, 17, 16)	(None, 14, 14, 16)	160
Convolutional	(None, 15, 15, 16)	(None, 12, 12, 16)	2320
Max-pooling	(None, 7, 7, 16)	(None, 6, 6, 16)	0
Dropout	(None, 7, 7, 16)	(None, 6, 6, 16)	0
Convolutional	(None, 5, 5, 32)	(None, 4, 4, 32)	4640
Convolutional	(None, 3, 3, 32)	(None, 2, 2, 32)	9248
Max-pooling	(None, 1, 1, 32)	(None, 1, 1, 32)	0
Dropout	(None, 1, 1, 32)	(None, 1, 1, 32)	0
Flatten	(None, 32)	(None, 32)	0
Dense	(None, 160)	(None, 160)	5280
Dropout	(None, 160)	(None, 160)	0
Dense	(None, 2)	(None, 2)	3

The data set used for diagnosis of SZ contains 16-channel EEG time series recorded at a sampling frequency of 128 Hz over 1 min, including F_7, F_3, F_4, F_8, T_3, C_3, C_z, C_4, T_4, T_5, P_3, P_z, P_4, T_6, O_1, and O_2. Notice that both data set come from studies of 16 common brain regions, with the AD data set having three more regions analyzed. Furthermore, it also includes two sets, (i) one of 39 healthy young individuals (control group; aged 11 to 14 years) and (ii) one of 45 teenagers individuals (aged 11 to 14 years) with symptoms of SZ.

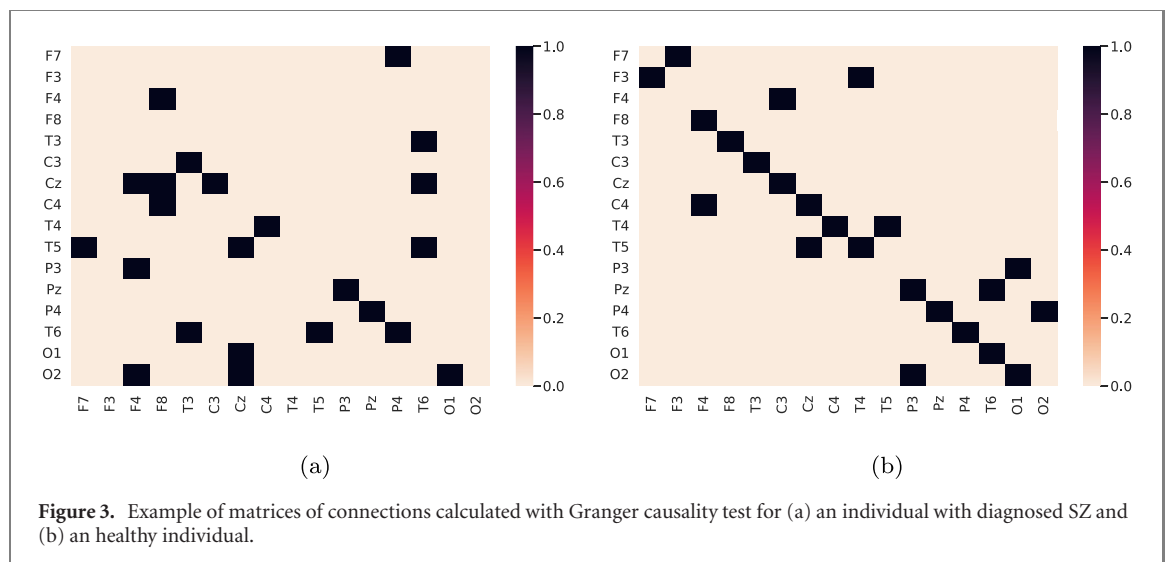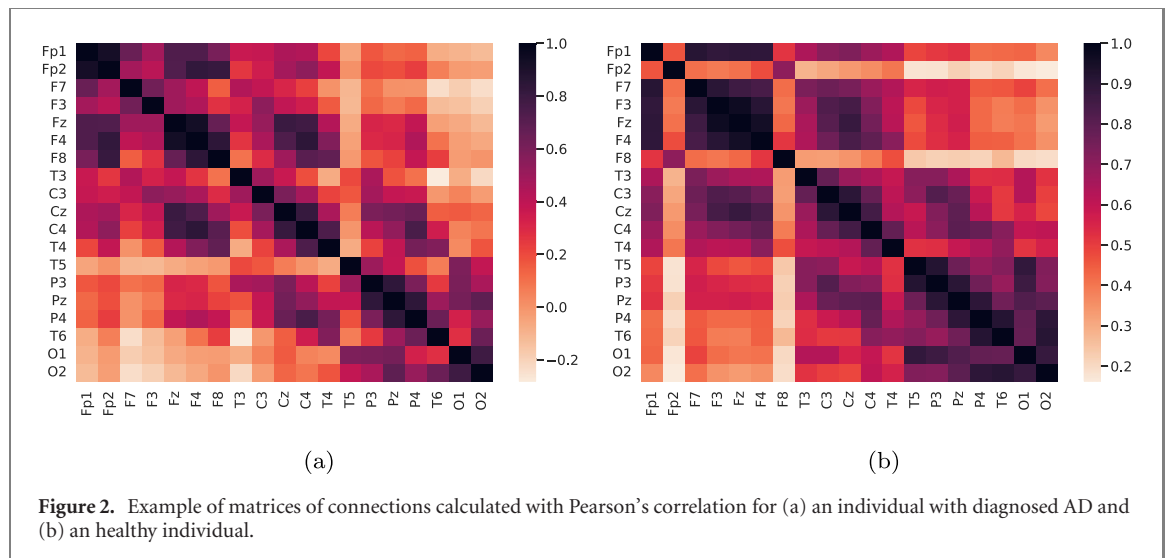The Alzheimer's disease database is freely available at [42].

3. Concepts and methods

Our framework to perform the automatic diagnosis of AD and SZ is illustrated in figure 1. In a first step, EEG time series, which are free of artifacts, are used to construct the matrices of connections. The strength of the connections between two brain regions is quantified by three different methods: (i) Granger causality test [43], (ii) the Pearson's [44] and (iii) Spearman's [45] correlation measures.

In our work, we have the following null hypothesis: the coefficients of the corresponding past values are zero (one EEG channel does not influence the other). The rows are the response variables and the columns are the predictors. We calculate the *p*-values, if these *p*-values are less than 0.05 (significance level) this implies

Table 3. The network architecture for the $CNN_{untuned}$ model used in the AD and SZ data sets.

Type of layer	Output layer (AD)	Output layer (SZ)	Kernel
Input layer	$19 \times 19 \times 1$	$16 \times 16 \times 1$	—
Convolution	$18 \times 18 \times 32$	$15 \times 15 \times 32$	4
Max pooling	$18 \times 18 \times 32$	$15 \times 15 \times 32$	2
Convolution	$17 \times 17 \times 16$	$14 \times 14 \times 16$	4
Max pooling	$17 \times 17 \times 16$	$14 \times 14 \times 16$	2
Flatten	$17 \times 17 \times 16$	3136	—
Fully connected	10	10	—
Fully connected	1	1	—

Figure 2. Example of matrices of connections calculated with Pearson's correlation for (a) an individual with diagnosed AD and (b) an healthy individual.

Figure 3. Example of matrices of connections calculated with Granger causality test for (a) an individual with diagnosed SZ and (b) an healthy individual.

that the null hypothesis can be rejected. Therefore, the p-value analyzes whether one brain region influences the other. If $p < 0.05$ we assign the value 1 because we reject the null hypothesis, i.e. it is true that one EEG channel influences another. This influence is related to having a high correlation.

Therefore, matrices are calculated for AD data sets (19 EEG channels) and for SZ data sets (16 EEG channels) filled with '1' if $p < 0.05$ and '0' if $p \geqslant 0.05$. These matrices are inserted in a CNN to discriminate healthy individuals from individuals diagnosed with AD and SZ (see figure 1). Notice that the use of different methods to infer the brain areas is necessary because there is no general method to infer functional connectivity [38–40, 46]. Indeed, choosing the best metric to infer these connections between brain areas is a current challenge in network neuroscience (e.g. [47, 48]).

Table 4. Classification results for AD using the CNN$_{tuned}$ model (best results are in bold).

Matrices of connections	Hyperparameter	Sample	Accuracy	Precision	Recall	AUC
	Random search	Train	0.81	0.81	0.81	0.88
		Test	0.75	0.75	0.75	0.97
	Hyper-band	Train	0.65	0.65	0.65	0.65
		Test	0.75	0.75	0.75	0.97
Granger causality	Bayesian optimization	Train	0.68	0.68	0.68	0.82
		Test	0.75	0.75	0.75	0.93
	Random search	Train	**0.95**	**0.95**	**0.95**	**0.98**
		Test	**1.00**	**1.00**	**1.00**	**1.00**
	Hyper-band	Train	0.86	0.86	0.86	0.90
		Test	1.00	1.00	1.00	1.00
Pearson's correlation	Bayesian optimization	Train	0.88	0.88	0.88	0.98
		Test	1.00	1.00	1.00	1.00
	Random search	Train	0.47	0.47	0.45	0.47
		Test	0.75	0.75	0.75	0.75
	Hyper-band	Train	0.47	0.47	0.47	0.45
		Test	0.75	0.75	0.75	0.62
Spearman correlation	Bayesian optimization	Train	0.47	0.47	0.47	0.45
		Test	0.75	0.75	0.75	0.68

Table 5. Classification results for SZ using the CNN$_{tuned}$ model (best results are in bold).

Matrices of connections	Hyperparameter	Sample	Accuracy	Precision	Recall	AUC
	Random search	Train	**0.90**	**0.90**	**0.90**	**0.93**
		Test	**1.00**	**1.00**	**1.00**	**1.00**
	Hyper-band	Train	0.73	0.73	0.73	0.77
		Test	0.72	0.72	0.72	0.78
Granger causality	Bayesian optimization	Train	0.72	0.72	0.72	0.78
		Test	1.00	1.00	1.00	1.00
	Random search	Train	0.54	0.54	0.54	0.54
		Test	0.50	0.50	0.50	0.50
	Hyper-band	Train	0.54	0.54	0.54	0.54
		Test	0.50	0.50	0.50	0.50
Pearson's correlation	Bayesian optimization	Train	0.54	0.54	0.54	0.54
		Test	0.50	0.50	0.50	0.50
	Random search	Train	0.53	0.53	0.53	0.53
		Test	0.50	0.50	0.50	0.50
	Hyper-band	Train	0.53	0.53	0.53	0.53
		Test	0.50	0.50	0.50	0.50
Spearman correlation	Bayesian optimization	Train	0.53	0.53	0.53	0.53
		Test	0.50	0.50	0.50	0.50

Table 6. Classification results for AD using the CNN$_{untuned}$ model (best results are in bold).

Matrices of connections	Sample	Accuracy	Precision	Recall	AUC
Granger causality	Train	0.97	0.97	0.99	0.99
	Test	0.58	0.57	0.66	0.75
Pearson's correlation	Train	**0.98**	**0.99**	**0.98**	**0.99**
	Test	**0.92**	**1.00**	**0.83**	**1.00**
Spearman's correlation	Train	0.97	0.98	0.97	0.99
	Test	0.83	1.00	0.66	1.00

3.1. Convolutional neural network

CNN is a type of neural network [49] with three types of layers and masked parameters, as proposed in [50, 51]. The convolutional layer performs the mathematical operation called convolution, which is done in more than one dimension at a time. The weights of the artificial neurons are represented by a tensor called kernel (or filter). The outputs from the convolutional layer include the main features from the input data. The convolution process between neurons and kernels produces outputs called feature maps.

Table 7. Classification results for SZ using the CNN$_{\text{untuned}}$ model.

Matrices of connections	Sample	Accuracy	Precision	Recall	AUC
Granger causality	Train	**0.97**	**0.97**	**0.97**	**0.99**
	Test	**0.52**	**0.53**	**0.73**	**0.55**
Pearson's correlation	Train	0.61	0.58	1.00	0.53
	Test	0.57	0.55	1.00	0.45
Spearman's correlation	Train	0.62	0.59	0.97	0.58
	Test	0.62	0.58	1.00	0.53

Table 8. Classification results for AD using raw EEG time series and the CNN$_{\text{tuned}}$ model.

Set	Accuracy	Precision	Recall	AUC
Train	0.68	0.61	1.00	0.68
Test	0.75	0.66	1.00	0.75

Table 9. Classification results for SZ using raw EEG time series and the CNN$_{\text{tuned}}$ model.

Set	Accuracy	Precision	Recall	AUC
Train	0.62	0.62	1.00	0.50
Test	0.55	0.55	1.00	0.50

The pooling layer reduces the dimensionality and operates similarly to the convolutional layer. The difference is that pooling kernels are weightless and add aggregation functions to their input data, such as a maximum or mean function [52, 53]. The max-pooling function is used here to return the highest value within an area of the tensor, which reduces the size of the feature map. The fully connected layer categorizes input data into different classes, based on an initial set of data used for training. The artificial neurons in the max pooling and fully connected layers are connected, as the output predicts precisely the result of the input EEG data as healthy and unhealthy [21].
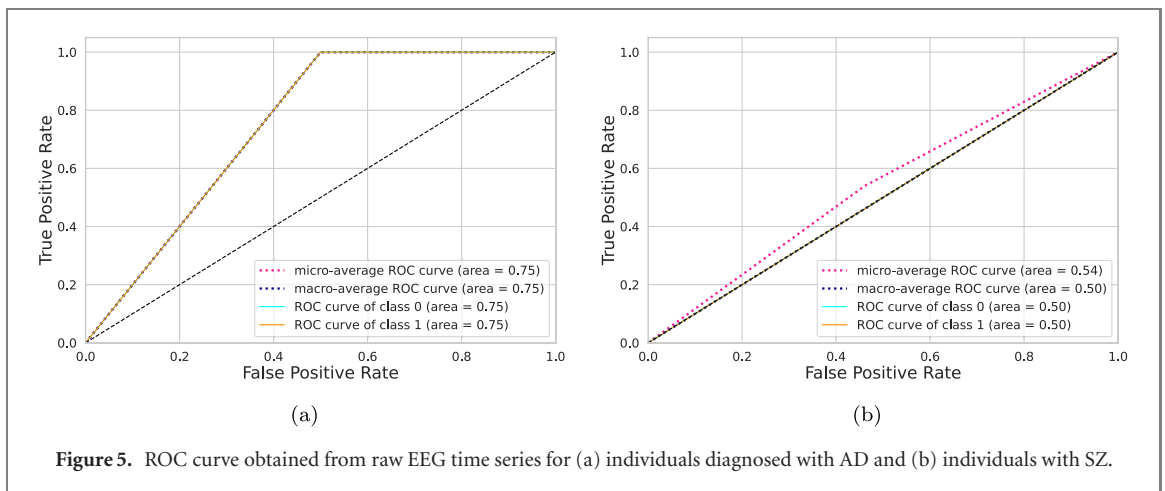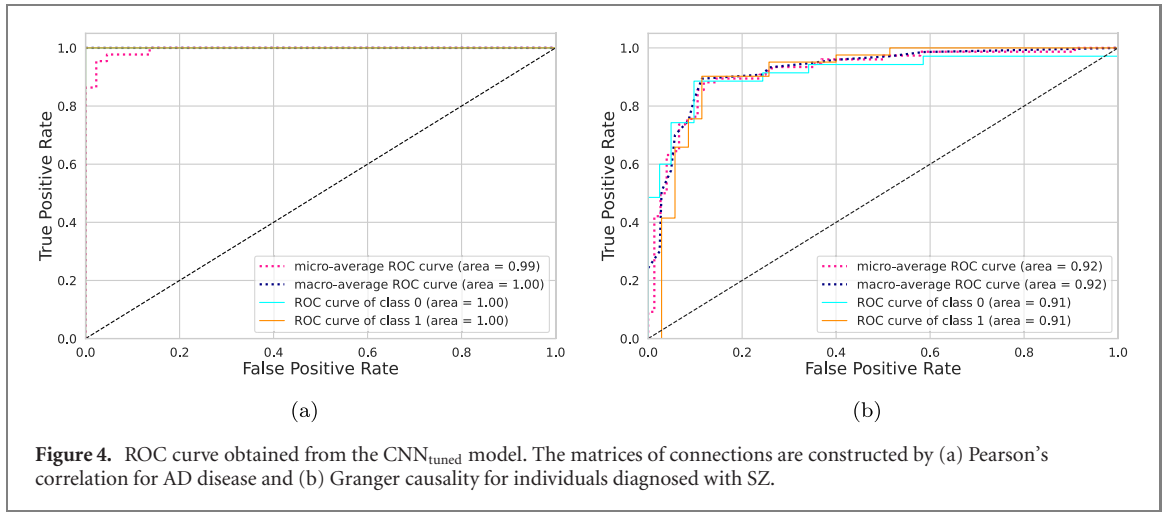
Two approaches for the CNN architectures are proposed here, one using a tuning method (CNN$_{\text{tuned}}$) and another without this optimization step (CNN$_{\text{untuned}}$). Tuning is an optimization method used to find the values of hyperparameters to improve the performance of the CNN model [54]. Three tuning techniques are used in the present work: (i) random search [55], (ii) hyper-band [56] and (iii) Bayesian optimization [57]. The traditional way to optimize the hyperparameters is exhaustive searching through a manually specified parameters search space and evaluating all possible combinations of these parameter values. However, this approach has a high computational cost. An alternative method is to select the values of parameters in the search space at random until maximize the objective function (here, this objective function is the maximization of accuracy).

The idea of hyper-band optimizations is to select different possible models (with different hyperparameters values), train them for a time, and discard the worst one at each iteration until a few combinations remain. In contrast, Bayesian optimization is a global optimization method that uses the Bayes theorem to direct the search to find the minimum or maximum of a certain objective function [30].

In the CNN$_{\text{tuned}}$ model, the dropout regularization technique is employed to avoid overfitting [58]. The layers and range used for hyperparameters are presented in table 1. The best CNN$_{\text{tuned}}$ architectures tuned for each data set individually are depicted in table 2. The CNN$_{\text{untuned}}$ model presents fewer layers and therefore lower computational costs. The parameters used in our analysis are described in table 3.

3.2. Evaluation

Since we have a two-class classification problem (negative and positive), we consider the precision and recall measures in the evaluation process [59]. Precision (also called specificity) corresponds to the hit rate in the negative class, whereas recall (also called sensitivity) measures how well a classifier can predict positive examples (hit rate in the positive class). For visualization of these two measures, the receiver operating characteristic (ROC) curve is a common method as it displays the relation between the rate of true positives and false positives. The area below this curve, called area under ROC curve (AUC) has been widely used in classification problems [60], mainly for medical diagnoses [61–64]. The value of the AUC varies from 0 to 1, where the value of one corresponds to a classification result free of errors. AUC = 0.5 indicates that the classifier is not able to distinguish the two classes—this result is equal to the random choice. Furthermore, we consider the macro

Figure 4. ROC curve obtained from the CNN$_{tuned}$ model. The matrices of connections are constructed by (a) Pearson's correlation for AD disease and (b) Granger causality for individuals diagnosed with SZ.

Figure 5. ROC curve obtained from raw EEG time series for (a) individuals diagnosed with AD and (b) individuals with SZ.

average of ROC curve, which computes the AUC metric independently for each class (calculate AUC metric for healthy individuals, class zero, and separately calculate for unhealthy subjects, class one) and then the average is computed considering these classes equally, in other words, an arithmetic mean is taken (the ROC curve of class 0 and the ROC curve of class 1 are calculated, summed and divided by 2). The micro average is also used in our evaluation, which does not consider both classes equally, but aggregates the contributions of the classes separately and then calculates the average. Therefore, the number of elements in each class is considered as weight in the calculation of the average.

4. Results and discussion

We consider the EEG time series described in section 2 to construct the matrices of connections for healthy controls and individuals diagnosed with AD and SZ, following the description in section 3. These matrices are built by using the Granger causality test, Pearson's and Spearman's correlations measures for both data sets. In figures 2 and 3, some examples of such matrices of connections are shown and differences between them can be noticed visually in both cases.

The matrices of connections are inserted into the CNN by applying the flattening method, which converts the data into a one-dimensional array that is input to the next layer. Two CNN architectures are considered, i.e. CNN$_{tuned}$ and CNN$_{untuned}$, to evaluate the classification. The CNN$_{tuned}$ is obtained by hyperparameter optimization, whereas the CNN$_{untuned}$ is a simpler model, without using the tuning optimization. The evaluation of both models is done by using the area under the ROC curve (AUC). Nested k-fold cross-validation ($k = 10$) for model selection, adjustment and evaluation is considered here. The training and test sets are selected according to the holdout method, where we include 10% of the observations in the test set. The training set is used to adjust the model, whereas the test set, for evaluation. Notice that these sets do not share any observations. We also perform the classification considering 10% to 50% of the observation in the test set and verify that

regardless of the sample size, the obtained AUC is higher than 0.90 in all cases. These results were included in the appendix, at the end of the paper.

The results for the CNN_{tuned} model is shown in tables 4 and 5, for AD and SZ, respectively. In all the cases, the CNN_{tuned} model can unambiguously distinguish healthy individuals from individuals diagnosed with a brain disorder. The best results with an accuracy close to 100% are obtained for both AD and SZ in the testing set using random search for hyperparameter tuning.

Concerning the $CNN_{untuned}$ model, the results are shown in tables 6 and 7 for AD and SZ, respectively. For the AD data set, the best results are found using Pearson's correlation with a test accuracy of 92%. Regarding SZ disease, independently of the method used for the construction of the matrices of connections, results are close to the random guessing (see table 7). Therefore, the CNN_{tuned} model is more accurate for both AD and SZ diagnosis.

Importantly, the overall predictive performance depends on the choice of measure to construct the matrices of connections. In the case of AD, Pearson's correlation provides the best performance in CNN_{tuned} (see table 4). On the other hand, in the case of SZ, Granger causality is superior to the other methods (see table 5). Therefore, there is no general method to infer the connections and obtain the most accurate results. Thus, different methods should be considered to develop an accurate framework for the automatic diagnosis of mental disorders.

For a comparison of our method with the more common approach known from the literature, the classification is performed by applying the raw EEG time series as input for the CNN_{tuned} model (whose performance is the best for both diseases, as discussed before). The results are shown in tables 8 and 9 for AD and SZ, respectively. The accuracy of 75% for AD and 55% for SZ are obtained. This outcome is supported by results available in the literature. Janghel and Rathore [65] obtained an accuracy of 76% for AD, where the authors did not consider the matrices of connections.

As we can see, our proposed method based on a matrix of connections provided as input to a CNN allows for more accurate results. This reinforces the importance of using a data set that encompasses the connections between brain regions. Indeed, the network structure is a fundamental ingredient to differentiate healthy individuals from patients presenting neurological disorders, as verified in many papers (e.g. [25, 66–69]).

In figure 4 we show the ROC curve for the best results, i.e. for AD (using Pearson's correlation) and SZ (using Granger causality test), respectively. For AD, the micro and macro-average ROC curve areas are 0.99 and 1.0, respectively, the micro and macro-average ROC curve areas are 0.92 for both cases. For comparison, figure 5 shows the ROC curve for AD and SZ using raw times series, where the micro and macro-average ROC curve areas are 0.75 for AD and around 0.55 for AZ. Comparing these results, we conclude that the use of the matrix of connections provides the most accurate classifications.

5. Conclusion

In this paper, we propose a method for automatic diagnosis of AD and SZ based on EEG time series and deep learning. We infer the matrix of connections between brain areas following three different approaches, based on Granger causality, Pearson's and Spearman's correlations. These matrices are included in a CNN, tunned with the random search, hyper-band, and Bayesian optimization. We verify that this approach provides a very accurate classification of patients with AD and SZ diseases. The comparison with the traditional method that considers raw EEG data shows that our method is more accurate, reinforcing the importance of network topology for the description of brain data. Our method is general and can be used for any mental disorder in which EEG times series can be recorded.

A limitation of our analysis is the relatively small data set, although this is common in other studies on disease classification [21]. However, even with this restriction, our algorithm worked very well, showing that AD and SZ are associated with changes in brain organization. As future work, we suggest considering larger data sets and additional information about the patients, like health conditions and age. A method that provides the level of the evolution of the disease is also an interesting topic to be developed from our study.

Acknowledgments

Table 10. Table containing the hyper-parameters for each classifier using the Grid search optimizer.

Classifier	Hyperparameters and description	Values
RF	-max_depth: the maximum depth of the tree -max_features: the number of features to consider when looking for the best split -min_samples_leaf: the minimum number of samples required to be at a leaf node -min_samples_split: the minimum number of samples required to split an internal node -n_estimators: the number of trees in the forest	[1, 2, 5, 10, 20, 80] [2, 3, 5, 10] [1, 2, 3, 4, 5] [1, 2, 8, 10, 12, 20] [1, 2, 3, 5, 10, 30, 50, 100, 200, 300, 500]
SVM	-kernel: specifies the kernel type to be used in the algorithm -gamma: kernel coefficient -C: regularization parameter	[rbf, linear] $[1 \times 10^{-3}, 1 \times 10^{-4}]$ [1, 10, 100, 1000]
NB	-var_smoothin: portion of the largest variance of all features that is added to variances for calculation stability	Range 1×10^{-9} to 1
MLP	-activation: activation function for the hidden layer -solver: the solver for weight optimization -alpha: L2 penalty (regularization term) parameter -batch_size: size of minibatches for stochastic optimizers -learning_rate: learning rate schedule for weight updates -learning_rate_init: the initial learning rate used	[identity, logistic, tanh, relu] [lbfgs, sgd, adam] $[0.0001, 1 \times 10^{-5}, 0.01, 0.001]$ [1000, 5000] [constant, invscaling, adaptive] [0.001, 0.01, 0.1, 0.2, 0.3]
XGBoost	-learning_rate: learning rate shrinks the contribution of each tree -min_samples_split: the minimum number of samples required to split an internal node -min_samples_leaf: the minimum number of samples required to be at a leaf node -max_depth: the maximum depth of the individual r egression estimators -max_features: the number of features to consider when looking for the best split -criterion: the function to measure the quality of a split -subsample: the fraction of samples to be used for fitting the individual base learners -n_estimators: the number of boosting stages to perform	[0.01, 0.025, 0.05, 0.075, 0.1, 0.15, 0.2] Range 0.1 to 0.5 Range 0.1 to 0.5 [3, 5, 8] [log2, sqrt] [friedman_mse, mae] [0.5, 0.618, 0.8, 0.85, 0.9, 0.95, 1.0] [10, 100. 1000, 10 000]

Table 11. Classification results for AD using the Pearson's correlation.

Classifier	Subset	AUC	Acc.	F1 score	Recall	Precision
SVM	Train	0.95	0.95	0.95	0.95	0.95
	Test	0.91	0.91	0.91	0.91	0.92
NB	Train	0.76	0.76	0.76	0.76	0.77
	Test	0.70	0.69	0.69	0.70	0.70
RF	Train	0.98	0.98	0.98	0.98	0.98
	Test	0.96	0.96	0.96	0.96	0.96
MLP	Train	1.00	1.00	1.00	1.00	1.00
	Test	0.97	0.97	0.97	0.97	0.97
GBC	Train	0.96	0.96	0.96	0.96	0.96
	Test	0.92	0.93	0.93	0.92	0.94

Table 12. Classification results for SZ using the Granger causality.

Classifier	Subset	AUC	Acc.	F1 score	Recall	Precision
SVM	Train	0.56	0.56	0.53	0.56	0.57
	Test	0.55	0.56	0.54	0.55	0.56
NB	Train	0.57	0.57	0.55	0.57	0.58
	Test	0.52	0.52	0.50	0.52	0.52
RF	Train	0.67	0.66	0.66	0.67	0.67
	Test	0.52	0.52	0.52	0.52	0.52
MLP	Train	0.64	0.63	0.60	0.64	0.72
	Test	0.59	0.59	0.56	0.59	0.61
GBC	Train	0.50	0.50	0.33	0.50	0.25
	Test	0.50	0.48	0.32	0.50	0.24
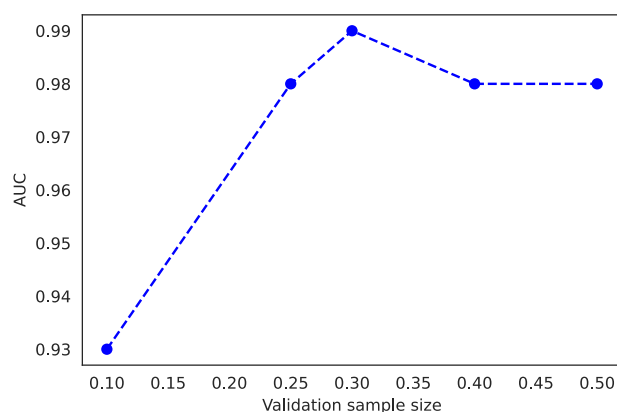
Figure 6. The AUC according to the test size for AD.

Data availability statement

The data that support the findings of this study are available upon reasonable request from the authors.

Appendix A. Machine learning algorithms for a small data set

Due to the fact that our data sets are very small since we cannot find more data in the available literature, and that CNN may suffer from this lack of data, in this section, we aim to try other classifiers that work more efficiently with small data sets.

For our best AD results using Pearson's correlation and SZ using Granger causality, we compared the following machine learning methods to classify: support vector machine (SVM) [70], random forest (RF) [71], naive Bayes (NB) [72], multilayer perceptron (MLP) [73] and extreme gradient boosting classifier [74] (XGBoost). We used the same resampling described used with CNN model with a hyperparametric optimization called grid search whose values used for each classifier model can be found in table 10.

We can see in the tables 11 and 12 the results of all classifiers and to AD (using the Pearson's correlation) and SZ (using the Granger causality), respectively. Note that there are no cases indicating overfitting. We can

observe in table 11 that all classifiers are able to differentiate between patients in different health conditions, as opposed to the results in table 12 that this cannot be verified (since all classifiers performed similarly to a random classifier). Therefore, CNN was able to differentiate both cases with better performance.

We also perform the classification considering 10% to 50% of the observation in the test set. Notice that we consider 10% of the elements in the test set to generate our results shown before. As we can see in figure 6, regardless of the sample size, the obtained AUC is higher than 0.90. We also included a k-fold cross-validation analysis for two different values of k, namely $k = 4$ and $k = 12$. For AD, considering $k = 4$, the AUC train is 0.99 and $k = 12$, the AUC train is 0.91. Therefore, we can see that we can predict the mental disorders with high accuracy, independent of the test size and using the k-fold cross-validation technique.

ORCID iDs

Francisco A Rodrigues https://orcid.org/0000-0002-0145-5571

References

[1] Levi-Montalcini R *et al* (W. H. Organization) 2006 *Neurological Disorders: Public Health Challenges* (Switzerland: World Health Organization)
[2] Dolgin E 2016 How to defeat dementia *Nature* **539** 156
[3] World Health Organization 2021 *Dementia* https://who.int/news-room/fact-sheets/detail/dementia (accessed 21 September 2021)
[4] Rodriguez S *et al* 2021 Machine learning identifies candidates for drug repurposing in Alzheimer's disease *Nat. Commun.* **12** 1033
[5] Jahmunah V, Lih Oh S, Rajinikanth V, Ciaccio E J, Hao Cheong K, Arunkumar N and Acharya U R 2019 Automated detection of schizophrenia using nonlinear signal processing methods *Artif. Intell. Med.* **100** 101698
[6] Gottesman I I and Shields J 1982 *Schizophrenia* (Washington: CUP Archive)
[7] World Health Organization 2021 *Schizophrenia* https://who.int/news-room/fact-sheets/detail/schizophrenia (accessed 21 September 2021)
[8] Borsboom D and Cramer A O J 2013 Network analysis: an integrative approach to the structure of psychopathology *Annu. Rev. Clin. Psychol.* **9** 91
[9] Fried E I, van Borkulo C D, Cramer A O J, Boschloo L, Schoevers R A and Borsboom D 2017 Mental disorders as networks of problems: a review of recent insights *Soc. Psychiatry Psychiatr. Epidemiol.* **52** 1
[10] Borsboom D 2008 Psychometric perspectives on diagnostic systems *J. Clin. Psychol.* **64** 1089
[11] Dauwels J, Vialatte F and Cichocki A 2010 Diagnosis of Alzheimer's disease from EEG signals: where are we standing? *Curr. Alzheimer Res.* **7** 487
[12] Jack C R *et al* 2009 Serial PIB and MRI in normal, mild cognitive impairment and Alzheimer's disease: implications for sequence of pathological events in Alzheimer's disease *Brain* **132** 1355
[13] Ding Y *et al* 2019 A deep learning model to predict a diagnosis of Alzheimer disease by using 18F-FDG PET of the brain *Radiology* **290** 456
[14] Walhovd K B *et al* 2010 Combining MR imaging, positron-emission tomography, and CSF biomarkers in the diagnosis and prognosis of Alzheimer disease *Am. J. Neuroradiol.* **31** 347
[15] Del Guerra A *et al* 2018 Trimage: a dedicated trimodality (PET/MR/EEG) imaging tool for schizophrenia *Eur. Psychiatr.* **50** 7
[16] Tait L *et al* 2020 EEG microstate complexity for aiding early diagnosis of Alzheimer's disease *Sci. Rep.* **10** 1
[17] Trambaiolli L R, Falk T H, Fraga F J, Anghinah R and Lorena A C 2011 EEG spectro-temporal modulation energy: a new feature for automated diagnosis of Alzheimer's disease *2011 Annual Int. Conf. IEEE Engineering in Medicine and Biology Society* (Piscataway, NJ: IEEE) pp 3828–31
[18] Falk T H, Fraga F J, Trambaiolli L and Anghinah R 2012 EEG amplitude modulation analysis for semi-automated diagnosis of Alzheimer's disease *EURASIP J. Adv. Signal Process.* **2012** 192
[19] Piubelli L, Pollegioni L, Rabattoni V, Mauri M, Cariddi L P, Versino M and Sacchi S 2021 Serum d-serine levels are altered in early phases of Alzheimer's disease: towards a precocious biomarker *Transl. Psychiatry* **11** 77
[20] Pineda A M, Ramos F M, Betting L E and Campanharo A S L O 2020 Quantile graphs for EEG-based diagnosis of Alzheimer's disease *PLoS One* **15** e0231169
[21] Oh S L, Vicnesh J, Ciaccio E J, Yuvaraj R and Acharya U R 2019 Deep convolutional neural network model for automated diagnosis of schizophrenia using EEG signals *Appl. Sci.* **9** 2870
[22] Ahmadlou M, Adeli H and Adeli A 2011 Fractality and a wavelet-chaos-methodology for EEG-based diagnosis of Alzheimer disease *Alzheimer Dis. Assoc. Disord.* **25** 85
[23] Buettner R, Beil D, Scholtz S and Djemai A 2020 Development of a machine learning based algorithm to accurately detect schizophrenia based on one-minute EEG recordings *Proc. 53rd Hawaii Int. Conf. System Sciences*
[24] Sporns O 2002 Network analysis, complexity, and brain function *Complexity* **8** 56
[25] de Arruda G F, Fontoura Costa L. d., Schubert D and Rodrigues F A 2014 Structure and dynamics of functional networks in child-onset schizophrenia *Clin. Neurophysiol.* **125** 1589
[26] Costa L d F, Rodrigues F A, Travieso G and Villas Boas P R 2007 Characterization of complex networks: a survey of measurements *Adv. Phys.* **56** 167
[27] Costa L d F, Villas Boas P R, Silva F N and Rodrigues F A 2010 A pattern recognition approach to complex networks *J. Stat. Mech.* P11015
[28] Diykh M, Li Y and Wen P 2017 Classify epileptic EEG signals using weighted complex networks based community structure detection *Expert Syst. Appl.* **90** 87

[29] La Rocca M, Garner R, Amoroso N, Lutkenhoff E S, Monti M M, Vespa P, Toga A W and Duncan D 2020 Multiplex networks to characterize seizure development in traumatic brain injury patients *Front. Neurosci.* **14** 1238

[30] Goodfellow I, Bengio Y and Courville A 2016 *Deep Learning* (Cambridge, MA: MIT Press)

[31] Acharya U R, Oh S L, Hagiwara Y, Tan J H and Adeli H 2018 Deep convolutional neural network for the automated detection and diagnosis of seizure using EEG signals *Comput. Biol. Med.* **100** 270

[32] Kashiparekh K, Narwariya J, Malhotra P, Vig L and Shroff G 2019 ConvTimeNet: a pre-trained deep convolutional neural network for time series classification *2019 Int. Joint Conf. Neural Networks (IJCNN)* (Piscataway, NJ: IEEE) pp 1–8

[33] Islam J and Zhang Y 2018 Brain MRI analysis for Alzheimer's disease diagnosis using an ensemble system of deep convolutional neural networks *Brain Inform.* **5** 2

[34] Duneja A, Puyalnithi T, Vankadara M V and Chilamkurti N 2019 Analysis of inter-concept dependencies in disease diagnostic cognitive maps using recurrent neural network and genetic algorithms in time series clinical data for targeted treatment *J. Ambient Intell. Humaniz. Comput.* **10** 3915

[35] Acharya U R, Oh S L, Hagiwara Y, Tan J H, Adeli H and Subha D P 2018 Automated EEG-based screening of depression using deep convolutional neural network *Comput. Methods Programs Biomed.* **161** 103

[36] Oh S L, Hagiwara Y, Raghavendra U, Yuvaraj R, Arunkumar N, Murugappan M and Acharya U R 2018 A deep learning approach for Parkinson's disease diagnosis from EEG signals *Neural Comput. Appl.* **32** 10927–33

[37] Yildirim Ö, Baloglu U B and Acharya U R 2018 A deep convolutional neural network model for automated identification of abnormal EEG signals *Neural Comput. Appl.* **32** 15857–68

[38] Bastos A M and Schoffelen J-M 2016 A tutorial review of functional connectivity analysis methods and their interpretational pitfalls *Front. Syst. Neurosci.* **9** 175

[39] Seth A K, Barrett A B and Barnett L 2015 Granger causality analysis in neuroscience and neuroimaging *J. Neurosci.* **35** 3293

[40] Bonita J D, Ambolode L C C, Rosenberg B M, Cellucci C J, Watanabe T A A, Rapp P E and Albano A M 2014 Time domain measures of inter-channel EEG correlations: a comparison of linear, nonparametric and nonlinear measures *Cogn. Neurodyn.* **8** 1

[41] Pritchard W S, Duke D W and Coburn K L 1991 Altered EEG dynamical responsivity associated with normal aging and probable Alzheimer's disease *Dement. Geriatr. Cogn. Disord.* **2** 102

[42] Pineda A *et al* 2020 Quantile graphs for EEG-based diagnosis of Alzheimer's disease *PLoS One* **15**

[43] Granger C W J 1969 Investigating causal relations by econometric models and cross-spectral methods *Econometrica* **37** 424

[44] Benesty J, Chen J, Huang Y and Cohen I 2009 Pearson correlation coefficient *Noise Reduction in Speech Processing* (Berlin: Springer) pp 1–4

[45] Lubinski D 2004 Introduction to the special section on cognitive abilities: 100 years after Spearman's (1904) ''general intelligence', objectively determined and measured' *J. Pers. Soc. Psychol.* **86** 96

[46] Comin C H, Peron T, Silva F N, Amancio D R, Rodrigues F A and Costa L d F 2020 Complex systems: features, similarity and connectivity *Phys. Rep.* **861** 1

[47] Shandilya S G and Timme M 2011 Inferring network topology from complex dynamics *New J. Phys.* **13** 013004

[48] Lusch B, Maia P D and Kutz J N 2016 Inferring connectivity in networked dynamical systems: challenges using Granger causality *Phys. Rev.* E **94** 032220

[49] Millstein F 2020 *Convolutional Neural Networks in Python: Beginner's Guide to Convolutional Neural Networks in Python* (South Carolina: Createspace Independent Publishing Platform)

[50] Hubel D H and Wiesel T N 1962 Receptive fields, binocular interaction and functional architecture in the cat's visual cortex *J. Physiol.* **160** 106

[51] López-Risueño G, Grajal J, Haykin S and Díaz-Oliver R 2002 Convolutional neural networks for radar detection *Int. Conf. Artificial Neural Networks* (Berlin: Springer) pp 1150–5

[52] LeCun Y *et al* 1989 Generalization and network design strategies *Connectionism in Perspective* vol 19 p 143

[53] LeCun Y, Bengio Y and Hinton G 2015 *Nature* **521** 436

[54] Hutter F, Lücke J and Schmidt-Thieme L 2015 Beyond manual tuning of hyperparameters *Künstl. Intell.* **29** 329

[55] Bergstra J and Bengio Y 2012 Random search for hyper-parameter optimization *J. Mach. Learn. Res.* **13** 1–25

[56] Rostamizadeh A, Talwalkar A, DeSalvo G, Jamieson K and Li L 2017 Efficient hyperparameter optimization and infinitely many armed bandits *5th Int. Conf. Learning Representations*

[57] Doke P, Shrivastava D, Pan C, Zhou Q and Zhang Y-D 2020 Using CNN with Bayesian optimization to identify cerebral micro-bleeds *Mach. Vis. Appl.* **31** 36

[58] Srivastava N, Hinton G, Krizhevsky A, Sutskever I and Salakhutdinov R 2014 Dropout: a simple way to prevent neural networks from overfitting *J. Mach. Learn. Res.* **15** 1929

[59] Maimon O and Rokach L 2010 *Data Mining and Knowledge Discovery Handbook* (Berlin: Springer)

[60] Jin Huang J and Ling C X 2005 Using AUC and accuracy in evaluating learning algorithms *IEEE Trans. Knowl. Data Eng.* **17** 299

[61] Ozcift A and Gulten A 2011 Classifier ensemble construction with rotation forest to improve medical diagnosis performance of machine learning algorithms *Comput. Methods Programs Biomed.* **104** 443

[62] Shen L, Chen H, Yu Z, Kang W, Zhang B, Li H, Yang B and Liu D 2016 Evolving support vector machines using fruit fly optimization for medical data classification *Knowl. Based Syst.* **96** 61

[63] Tanwani A K, Afridi J, Shafiq M Z and Farooq M 2009 Guidelines to select machine learning scheme for classification of biomedical datasets *European Conf. Evolutionary Computation, Machine Learning and Data Mining in Bioinformatics* (Berlin: Springer) pp 128–39

[64] Nanni L, Lumini A and Brahnam S 2010 Local binary patterns variants as texture descriptors for medical image analysis *Artif. Intell. Med.* **49** 117

[65] Janghel R R and Rathore Y K 2021 Deep convolution neural network based system for early diagnosis of Alzheimer's disease *IRBM* **42** 258

[66] Lynn C W and Bassett D S 2019 The physics of brain network structure, function and control *Nat. Rev. Phys.* **1** 318

[67] De Vico Fallani F, Rodrigues F A, da Fontoura Costa L, Astolfi L, Cincotti F, Mattia D, Salinari S and Babiloni F 2011 Multiple pathways analysis of brain functional networks from EEG signals: an application to real data *Brain Topogr.* **23** 344

[68] Rodrigues F A and da Fontoura Costa L 2009 A structure-dynamic approach to cortical organization: number of paths and accessibility *J. Neurosci. Methods* **183** 57

[69] Antiqueira L, Rodrigues F A, van Wijk B C M, Costa L d F and Daffertshofer A 2010 Estimating complex cortical networks via surface recordings—a critical note *Neuroimage* **53** 439

[70] Bottou L and Lin C-J 2007 *Support Vector Machine Solvers* (Cambridge, MA: MIT Press)

[71] Breiman L 2001 Random forests *Mach. Learn.* **45** 5

[72] Friedman N, Geiger D and Goldszmidt M 1997 Bayesian network classifiers *Mach. Learn.* **29** 131

[73] Hinton G, Rumelhart D and Williams R 1986 Learning internal representations by error propagation *Parallel Distributed Processing: Explorations in the Microstructure of Cognition: Foundations* (Cambridge, MA: MIT Press)

[74] Friedman J H 2001 Greedy function approximation: a gradient boosting machine *Ann. Stat.* **29** 1189